



HAL
open science

Thermodynamical equilibrium for nuclear matter produced in heavy ion collisions around 100 AMeV?

B. Borderie, F. Gulminelli, M F. Rivet, L. Tassan-Got, M. Assenard, G. Auger, Co. Bacri, J. Benlliure, E. Bisquer, R. Bougault, et al.

► **To cite this version:**

B. Borderie, F. Gulminelli, M F. Rivet, L. Tassan-Got, M. Assenard, et al.. Thermodynamical equilibrium for nuclear matter produced in heavy ion collisions around 100 AMeV?. International Conference on Nuclear Reaction Mechanisms 8, Jun 1997, Varenna, Italy. pp.239-248. in2p3-00003708

HAL Id: in2p3-00003708

<https://hal.in2p3.fr/in2p3-00003708>

Submitted on 28 Sep 1999

HAL is a multi-disciplinary open access archive for the deposit and dissemination of scientific research documents, whether they are published or not. The documents may come from teaching and research institutions in France or abroad, or from public or private research centers.

L'archive ouverte pluridisciplinaire **HAL**, est destinée au dépôt et à la diffusion de documents scientifiques de niveau recherche, publiés ou non, émanant des établissements d'enseignement et de recherche français ou étrangers, des laboratoires publics ou privés.

16 septembre 1997

CERN LIBRARIES, GENEVA



SCAN-9712057

IPNO-DRE-97-20
GANIL P 97 22
LYCEN/9726

CEA/DAPNIA/SPhN 97-32
LPCC 97-12
SUBATECH-97-18

***THERMODYNAMICAL EQUILIBRIUM FOR NUCLEAR
MATTER PRODUCED IN HEAVY ION COLLISIONS
AROUND 100 AMeV ?***

B. Borderie, F. Gulminelli, M.F. Rivet, L. Tassan-Got et al

*Invited talk to the 8th Int. Conf. on Nuclear Reactions
Mechanisms, Varenna (Italy), June 9-14, 1997*

THERMODYNAMICAL EQUILIBRIUM FOR NUCLEAR MATTER PRODUCED IN HEAVY ION COLLISIONS AROUND 100 AMeV ?

B. Borderie¹, F. Gulminelli², M.F. Rivet¹, L. Tassan-Got¹,
M. Assenard⁶, G. Auger³, Ch.O. Bacri¹, J. Benlliure³, E. Bisquer⁴, R. Bougault²,
F. Bocage², R. Brou², P. Buchet⁵, J.L. Charvet⁵, A. Chbihi³, J. Colin², D. Cussol²,
R. Dayras⁵, E. De Filippo⁵, A. Demeyer⁴, D. Doré¹, D. Durand², Ph. Eudes⁶, J.D.
Frankland¹, E. Galichet⁴, E. Genouin-Duhamel², E. Gerlic⁴, M. Germain⁶, D.
Gourio⁶, D. Guinet⁴, P. Lautesse⁴, J.L. Laville⁶, J.F. Lecomte², A. Le Fèvre³, T.
Lefort², R. Legrain⁵, O. Lopez², M. Louvel², N. Marie³, V. Métivier^{2a}, L. Nalpas⁵,
A.D. Nguyen², M. Parlog⁷, J. Péter², E. Plagnol¹, A. Rahmani⁶, T. Reposeur⁶, E.
Rosato^{3b}, S. Salou³, F. Saint-Laurent³, M. Squalli¹, J.C. Steckmeyer², M. Stern⁴, G.
Tabacaru⁷, B. Tamain², O. Tirel³, E. Vient², C. Volant⁵, J.P. Wieleczko³

¹ *Institut de Physique Nucléaire, IN2P3-CNRS, 91406 Orsay Cedex, France*

² *LPC, IN2P3-CNRS, ISMRA et Université, 14050 Caen Cedex, France*

³ *GANIL, CEA, IN2P3-CNRS, B.P. 5027, 14021 Caen Cedex, France*

⁴ *IPN Lyon, IN2P3-CNRS et Université, 69622 Villeurbanne Cedex, France*

⁵ *CEA, DAPNIA/SPhN, CEN Saclay, 91191 Gif sur Yvette Cedex, France*

⁶ *SUBATECH, IN2P3-CNRS et Université, 44072 Nantes Cedex 03, France*

⁷ *Inst. of Physics and Nuclear Eng., IFA, P.O. Box MG6, Bucharest, Romania.*

Vaporization events, where all species have atomic numbers lower than 3, resulting from binary dissipative collisions between ³⁶Ar and ⁵⁸Ni have been detected with high efficiency with the multidetector INDRA. Kinematical properties and chemical composition (mean values and variances) of vaporizing sources are derived over the excitation energy per nucleon range 8-28 MeV. Despite very unfavourable conditions (binary collisions with short reaction times and source life times), the properties of these vaporized sources are in agreement with the results of a model describing a gas of fermions and bosons in thermal and chemical equilibrium. This strongly suggests that thermodynamical equilibrium has been reached in such sources.

1 Introduction

The question of whether or not hot nuclear matter formed in violent heavy-ion collisions reaches thermodynamical equilibrium (thermal+chemical) before starting to disassemble is of essential importance in validating the hypotheses assumed in statistical models^{1,2,3} and in constraining the ingredients entering microscopic models based on transport theories^{4,5,6,7}. Moreover a positive an-

^apresent address: *SUBATECH, IN2P3-CNRS et Université, 44072 Nantes Cedex 03, France*

^bpermanent address: *Dipartimento di Scienze, Univ. di Napoli, 80125 Napoli, Italy*

swer to this question renders appropriate the application of physical concepts borrowed from macroscopic statistical mechanics like phase coexistence and phase transition. In order to study nuclear thermodynamics one needs to be able to univocally associate the detected reaction products with the thermodynamical variables (temperature, density) of the decaying source. At low excitation energies this aim is accomplished by the statistical model for surface evaporation (liquid-like phase of ordinary matter). At higher excitation energies the opening of channels like multifragmentation or vaporization which correspond to volume emission associated with final state interaction makes increasingly difficult both the experimental and theoretical situations.

From a theoretical point of view, if we limit our attention to light fragments without states in the continuum, we expect that at high temperature the high lying discrete levels will be increasingly excited. Since most of these states are particle unstable, their population can significantly modify the light particle yields and energy spectra. Another difficulty raises from the fact that in statistical model calculations the assumption is commonly taken that the multifragmentation pattern can be calculated in a non interacting freeze-out configuration. However, even in the framework of thermodynamical equilibrium, final state interactions at freeze-out can modify the production yields⁸.

The experimental study requires the detection and identification (mass and charge) of all or nearly all deexcitation products. This kind of measurement was recently achieved by studying with INDRA⁹ a particular class of events produced in $^{36}\text{Ar} + ^{58}\text{Ni}$ collisions, namely the vaporization events¹⁰. These events, where more than 90% of the charged particles were detected and isotopically identified, were properly characterized since the total number of - unmeasured - neutrons could be derived event by event from mass conservation. The vaporization events, which were studied at 52,74,84 and 95 AMeV incident energies, are produced in binary dissipative collisions. At the higher bombarding energy a broad excitation energy range (8-28 AMeV) is observed for the two partners of collisions (quasi projectile: QP and quasi target: QT)¹¹. Thus, the possible occurrence of thermodynamical equilibrium for such sources can be studied in a priori very unfavourable conditions (conservation of the binary character of collisions and very large excitation energies involved associated with short interaction and deexcitation times).

2 Properties of vaporizing sources

2.1 Excitation energies

To correctly derive the properties of these sources, the dynamics of the collisions must first be studied: are we dealing with the vaporization of one source,

or of several sources? The details given in ¹¹ indicate the dominance of collisions with two partners in the exit channel. Only a very small part of the events (whatever the incident energy) could possibly be associated with the decay of a single source and was not included in the analysis. Usually, for heavy systems, the source reconstruction makes use of the heaviest products only. In a similar way, the subset of particles with masses larger than 2 was used here. These particles carry on average more than 50% of the total mass of the system. Different methods (see ¹¹) were used to determine the source velocities and it was verified that they yield similar results; the spectra of the relative velocity between the sources were found very broad.

The primary masses and the excitation energies of the two sources were obtained by first including the measured particles not considered in the reconstruction of the sources (p and d); they were attributed to the source in which their relative velocity is smallest. Then, each event was completed in charge according to the measured particle distribution, and all added charged particles were attributed to the slower source, assuming that the effects of the detection thresholds overcome those of the geometrical efficiency. Finally total neutron multiplicity then follows from mass conservation; the forward source was completed to $N = Z + 1$ whenever its measured neutron number was smaller, the remaining neutrons were put in the backward source. The kinetic energies of the added charged particles were taken equal to the average energy of the same particle species in the events belonging to the same excitation energy bin; for neutrons one uses the average proton energy minus 2 MeV to take into account a Coulomb effect. At all energies, the source masses were found to be close (38 and 56) to the initial projectile and target masses but with large fluctuations ($\sigma \sim 8$). In the following the sources will then be called quasi-projectile (QP) and quasi-target (QT). The excitation energy of each source is calculated as ¹²

$$E_S^* = \sum_i (\Delta m_i + E_{Ki}) - \Delta m_S, \quad (1)$$

Δm_i being the mass excess of particle i , Δm_S that of the source, and E_{Ki} the i th particle kinetic energy in its source frame. As expected from the broad spectra observed for the relative velocities between the sources and for the QP and QT masses, the distributions of the excitation energy per nucleon of each source are also very broad. We can estimate at 2 A MeV the resolution of the calculated excitation energy per nucleon.

2.2 Kinematical properties and composition

Whether or not each vaporizing source reaches thermal or thermodynamical (thermal and chemical) equilibrium before disintegrating can be investigated by looking at the energy spectra and relative abundances of the different particles in each source¹³, as a function of its excitation energy per nucleon, ϵ^* ; a binning $\delta\epsilon^*=3\text{MeV}$ was chosen. We discuss first the shapes of the kinetic energy spectra, in the source frames, which give information about thermal equilibrium for each source.

First it was checked that the forward and backward spectra are superimposable¹⁴. Spectra, integrated over angle, are structureless, with exponential tails whose slopes are similar within 30% for all particles. More quantitatively, for the emission from a source in thermal equilibrium, all particles should have the same average kinetic energy if we neglect in a first approximation the Coulomb effect. The increase of the average kinetic energy with the excitation energy is almost linear for all particles¹³. An example of the evolution of the average kinetic energy of each particle species is given in Fig 1 (bottom part), for the QP at $\epsilon^*=18.5\text{ MeV}$ (identical values are obtained for the QT); a difference of $\sim 20\%$ is observed here and exists over the whole excitation energy range between the more energetic particles (d and ${}^3\text{He}$) and the less energetic ones (p,t and ${}^4\text{He}$). This may appear as a significant deviation from thermal equilibrium. However the role of quantal effects and side-feeding has to be checked. Note that no extra collective expansion energy (proportional to the atomic mass) can be derived from the data.

In Fig 1 (upper part) is shown the relative particle abundance ($P_j = M_j/M_S$, where M_S is the total source multiplicity and M_j the multiplicity of particle species j in the source) versus the source excitation energy, for the QP at 95 A MeV. α -particles dominate at the lower excitation energies, while nucleons take over when the excitation energy is increased. The deuteron relative abundance is roughly constant; the isobars of mass 3 have opposite behaviours: tritons slightly decrease and ${}^3\text{He}$ slightly increase when raising the energy. Finally the rare ${}^6\text{He}$ behave like the α 's. Note that for a given ϵ^* the relative yields are the same for the QP and the QT, independently of the bombarding energy.

In the data presented here, the sources were reconstructed without attempt to separate mid-rapidity emission¹⁵. It was checked that for these vaporization events the observables discussed in this section are negligibly affected by this approximation.

$^{36}\text{Ar} + ^{58}\text{Ni}$ $E/A=95$ MeV - QP vaporization

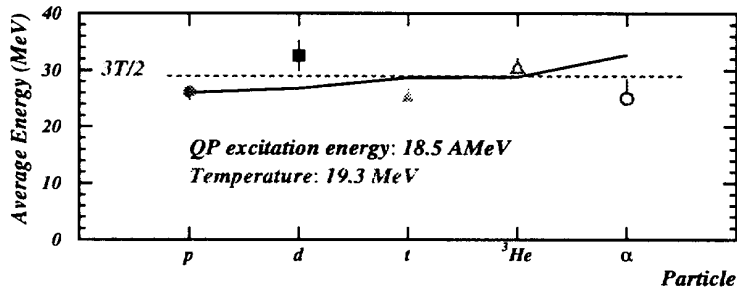
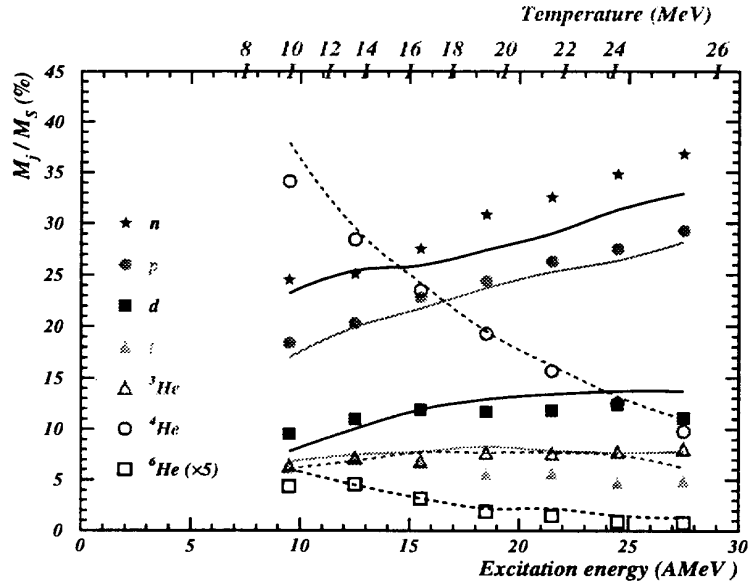


Figure 1: Bottom part: average kinetic energies of particles emitted by the QP with an excitation energy per nucleon of 18.5 MeV. The dashed line refers to the average kinetic energy of particles expected for an ideal gas at the temperature derived from the model. Upper part: composition of the QP as a function of its excitation energy. Symbols are for data while the lines are the results of the model. The temperature values used in the model are also given (see text).

2.3 Comparison with a chemical and thermal equilibrium fireball model

The physical scenario described in this section is a chemically and thermally equilibrated nuclear source which undergoes a simultaneous disassembly at a fixed temperature T and density ρ ¹⁶.

2.3.1 Mean energies of particles and chemical composition

In the proposed model¹⁷, the emitting source is viewed as a nuclear gas of fermions and bosons in thermal and also chemical equilibrium. For a given source density ρ and temperature T , the energy spectra $n_i(E)$ of the different nuclear species (and consequently their relative yields) are uniquely determined from conservation laws and the equilibrium distributions in the grandcanonical ensemble

$$n_i(E) = f_Q(E, \mu_i, T) \quad i = 1, \dots, N. \quad (2)$$

N is the number of species taken into account (limited here to all known discrete levels of nuclear species¹⁸ up to ^{20}Ne which deexcite in $Z=0,1,2$). In this formalism the discrete levels of the different isotopes are treated as independent structureless particles characterized by an internal energy augmented with respect to the ground state binding energy, and by their proper degeneracy factor. This corresponds to the implicit assumption that these states are sufficiently narrow, i.e. their life time is much longer than the equilibration time. Thus in the calculation only levels with widths equal to or lower than 2MeV are included in the state sum. f_Q is the density of occupied states taking into account the appropriate quantum statistics (Fermi or Bose) and μ_i is the chemical potential of the species i , which is a function of the break up density ρ via the neutron and proton chemical potentials μ_N, μ_Z

$$\mu_i = \mu_N N_i + \mu_Z Z_i + B_i \quad (3)$$

Here, N_i, Z_i are the neutron and proton numbers of the isotope under consideration and B_i its binding energy. At this point of the model the nuclear gas is ideal, i.e. the different species do not interact. This assumption is not correct since the freeze-out volume is not much larger than the proper volume of the nuclei and particles. Then corrections to an ideal gas are included in the form of excluded volume effects in the spirit of the Van der Waals gas to deal with collisions and reabsorption at freeze-out. The consequence of the excluded volume is to favour protons, neutrons and alphas over the more loosely bound structures like deuterons and high-lying resonances. Finally the calculated distributions are corrected for the side-feeding of resonance decay. In this calculation ε^* is derived, as in the experiment, by summing the kinetic energies of all particles and the Q value. The experimental ε^* range is covered

by varying T from 10 to 25 MeV. The freeze-out density has been fixed to $\rho = \rho_0/3$, in order to reproduce the experimental ratio between the proton and alpha yields. The results of the model correspond to the lines in Fig 1.

The average kinetic energies of the different particles are rather well reproduced over the whole excitation energy range¹⁹, particularly for ${}^3\text{He}$, but the model fails to accurately follow the dependence on the different species (see Fig 1 bottom). The energy differences between particles in the model are due to the different statistics (Fermi or Bose) and to side-feeding. This last effect, which depends on the number of species included in the model, does not influence much the calculated values¹⁴. The dashed line in Fig 1 (bottom) indicates the average kinetic energy, $(3/2 T)$, expected for an ideal gas. Experimental error bars in the figure give the limits obtained when different methods for reconstructing the sources are applied.

The yields of the different species as a function of the excitation energy (see Fig 1 top) are very well reproduced .

As indicated earlier, in this calculation the freeze-out density has been fixed to one third of the saturation density, the cut-off width of resonances is 2MeV and correction to an ideal gas are included. In order to obtain this degree of agreement with the data the correction to an ideal gas is very important: in the ideal gas case, the experimental proton over deuteron ratio would be fitted only by imposing a freeze-out density so low that the proton over alpha ratio would be overestimated by more than an order of magnitude¹⁷. Secondary decays contribute especially to the alpha and proton yields but the influence of the cut-off width of resonances is almost within the experimental error bars. The slight but systematic overestimation of the alpha kinetic energies observed seems to indicate that the yield from resonances is relatively low since secondary decays tend to increase the average energy of alpha particles. This does not mean that side feeding effects from particle decaying states can be neglected. Even with the suppression effect of the excluded volume interaction and with a very low cut-off width, side feeding plays a very important role especially on alpha particles: the majority of alphas come from secondary decays (see¹⁹).

The last parameter to be discussed is the freeze-out density, which is the only critical parameter of the model. A change in the density only very slightly affects the kinetic energies, but produces a sizeable modification in the production yields. Protons and deuterons are increasingly favoured over alphas as the density increases. Since no principle reason can be invoked to choose the density within 20% or even 50%, other observables independent of the mean multiplicities have to be considered before one can convincingly state that thermodynamical equilibrium has been reached. To this aim we have compared the second moments of the distributions, namely the variances of the particle

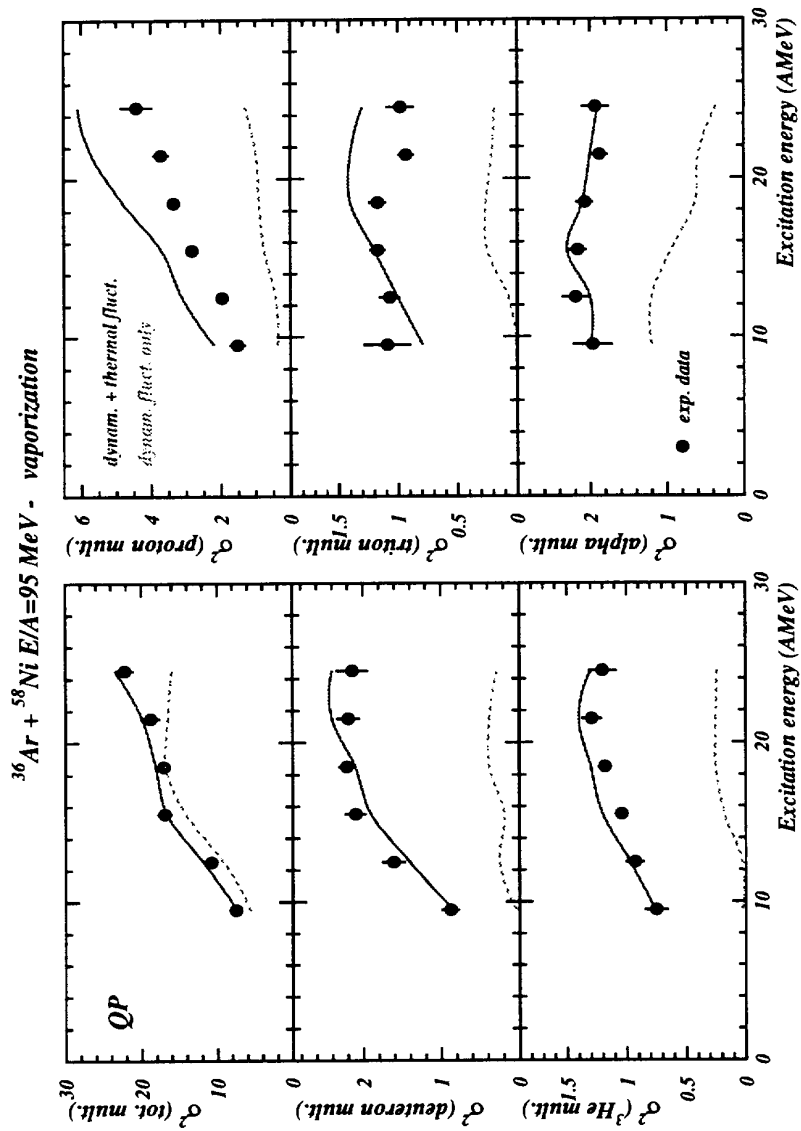


Figure 2: Variances of multiplicity distributions (total, proton, deuteron, triton, ^3He and alpha) of the QP as a function of its excitation energy per nucleon. Points refer to the data and the lines are the results of the model (see text).

multiplicities.

2.3.2 Variances of the multiplicity distributions

In principle variances can be analytically calculated as well as mean values in the grandcanonical ensemble. These variances originate from the random exchanges of particles and energy with the thermal bath. However it is experimentally observed that no thermal equilibrium is achieved between the two partners of the reaction, due to short reaction time^{11,20}. This means that the QT cannot be considered as a thermal bath for the QP, and that the observed fluctuations in mass and excitation energy of the sources have a dynamical origin. Therefore the variances of the multiplicities will have, together with a thermal component, a non equilibrated contribution coming from mass and energy fluctuations for sources (primary partners of collisions). In order to get rid of this non equilibrium component, the widths of the measured mass and excitation energy distributions of the source were used as inputs of the statistical calculation. A Monte Carlo simulation allows, with a temperature range such as to cover the experimental excitation energy range, to generate events from the grandcanonical probabilities with mass and excitation energy distributions of the source which reproduces experimental data. The comparison data-calculations is displayed in Fig 2 for the variances associated with the total multiplicity and with the different charged particle multiplicities. The order of magnitude is correctly reproduced by the calculation, as well as the evolution with the excitation energy. The thermal origin of the observed fluctuations is confirmed by a simulation (dashed curves) where, at each excitation energy, the statistical fluctuations are frozen (i.e. the partitions are fixed) and only the mass of the source is allowed to vary with a width fixed by the experimental distribution; as expected only variances on the total multiplicity are reproduced and the resulting dynamical fluctuations observed for the different particles cannot reproduce the experimental variations. The correct prediction of the measured variances validates the value of the freeze-out density fixed in the model and reinforces the idea that thermodynamical equilibrium has been reached.

3 Conclusions

Emission properties of vaporizing sources produced in collisions between ^{36}Ar and ^{58}Ni have been studied in a broad excitation energy range. The yields (mean values and variances) and the energy spectra of the different species have been compared with the predictions of a model describing the properties of a quantum weakly interacting gas of nuclear species in thermal and chemical equilibrium. All these experimental observables are rather well reproduced,

which give strong confidence in the fact that thermodynamical equilibrium has been reached even for these sources produced in very extreme conditions. Comparisons of this model with experimental data extended to caloric curves and temperature measurements^{19,21} confirmed the hypothesis developed in this paper. The model fails to reproduce data for excitation energy lower than 8-10 A MeV.

References

1. J. Bondorf et al, *Nucl. Phys.* **A443** (1985) 321, **A444** (1985) 460, **A448** (1986) 753.
2. D.H.E. Gross, *Rep. Prog. Phys.* **53** (1990) 605. and references therein
3. H. Stocker and W. Greiner, *Phys. Rep.* **5** (1986) 277
J. Konopka et al, *Phys. Rev.* **C50** (1994) 2085.
4. G. Bertsch and S. Das Gupta, *Phys. Rep.* **160** (1988) 189.
5. J. Aichelin, *Phys. Rep.* **202** (1991) 233.
6. A. Bonasera, F. Gulminelli, J. Molitoris, *Phys. Rep.* **243** (1994) 1.
7. D. Idier et al, *Ann. Phys. Fr.* **19** (1994) 159.
8. J. A. Lopez and J. Randrup, *Nucl. Phys.* **A503** (1989) 183.
9. J. Pouthas et al, *Nucl. Instr. Meth. in Phys. Res.* **A357** (1995) 418, **A369** (1996) 222.
10. C.O. Bacri et al, *Phys. Lett.* **B353** (1995) 27.
11. M.F. Rivet et al, *Phys. Lett.* **B388** (1996) 219.
12. D. Cussol et al, *Nucl. Phys.* **A561** (1993) 298.
13. B. Borderie et al, *Phys. Lett.* **B388** (1996) 224.
14. B. Borderie et al, Proc. of the Int. Workshop on H.I. Physics with 4 π detectors, Poiana Brasov, Romania, October 1996, World Scientific in press.
15. J. Péter et al, Proc. of the Int. Workshop on H.I. Physics with 4 π detectors, Poiana Brasov, Romania, October 1996, World Scientific in press.
16. A. Z. Mekjian, *Phys. Rev.* **C17** (1978) 1051
S. Das Gupta and A. Z. Mekjian, *Phys. Rep.* **72** (1981) 131.
17. F. Gulminelli and D. Durand, *Nucl. Phys.* **A615** (1997) 117.
18. J. Konopka, private communication; F. Ajzenberg-Selove, *Nucl. Phys.* **A320,449,475,506,521,564** (1979-1993).
19. F. Gulminelli et al, Proc. of the Int. Winter Meeting on Nuclear Physics, Bormio, Italy, February 1997, p 396.
20. B. Borderie et al, *Z. Phys A hadrons and nuclei* **357** (1997) 7
21. Y.G. Ma et al, *Phys. Lett.* **B390** (1997) 41.